

# Ionization and Abundances in Intrinsic QSO Absorption-Line Systems

F. Hamann, T. Barlow, R.D. Cohen, V. Junkkarinen & E.M. Burbidge

*Center for Astrophysics & Space Sciences, University of California –  
San Diego, La Jolla, CA, 92093-0424*

**Abstract.** We discuss two aspects of the ionization and abundances in QSO intrinsic absorbers. First, we use the high-ionization doublet Ne VIII  $\lambda\lambda 770,780$  to test the relationship between the UV line absorbers and the “warm” absorbers detected in soft X-rays. In one well-measured QSO with intrinsic  $z_a \approx z_e$  lines, UM 675, we estimate that the UV absorber has at least 10 times too little O VII and O VIII to produce the requisite bound-free edges at  $\sim 0.8$  keV. Second, we show that firm lower limits on the metal-to-hydrogen abundances can be established even with no constraints on the ionization. Those lower limits are typically  $Z \gtrsim Z_\odot$  and sometimes  $Z \gtrsim 10 Z_\odot$  (e.g. for the BALs). We argue that QSO metallicities up to at least  $\sim 9 Z_\odot$  are consistent with the rapid early epoch star formation expected in the cores of massive galaxies.

## 1. General Introduction

Intrinsic QSO absorption lines include the broad absorption lines (BALs), at least some of the much narrower associated ( $z_a \approx z_e$ ) lines, and any other ( $z_a \ll z_e$ ) systems that form near the QSO engine. We are involved in a program to identify these systems and study their kinematics, ionization and metal abundances using spectra from the *Hubble Space Telescope* (*HST*) and the Keck and Lick Observatories. Some results on the identifications and kinematics are discussed in the accompanying paper by Hamann *et al.* in this volume (hereafter Paper1).

## 2. Ne VIII and the UV Line–X-ray Warm Absorber Connection

The combined UV (*HST*) and visible (ground-based) spectra allow us to (1) measure lines across a wide range of ionizations and (2) derive reliable column densities from the relatively low-resolution *HST* spectra. We are particularly interested in the O VI  $\lambda\lambda 1032,1037$  and Ne VIII  $\lambda\lambda 770,780$  doublets to probe the high-ionization gas and test the possible relationship (Mathur *et al.* 1994; also Mathur *et al.* and Shields & Hamann this volume) between the UV-line and X-ray warm absorbing regions. Warm absorbers can be identified by bound-free absorption edges of O VII and/or O VIII at  $\sim 0.8$  keV. Measurements of the Ne VIII column density can directly constrain the amount of warm absorber material because O VII and O VIII are the dominant species of oxygen in the Ne VIII absorbing gas (see below).

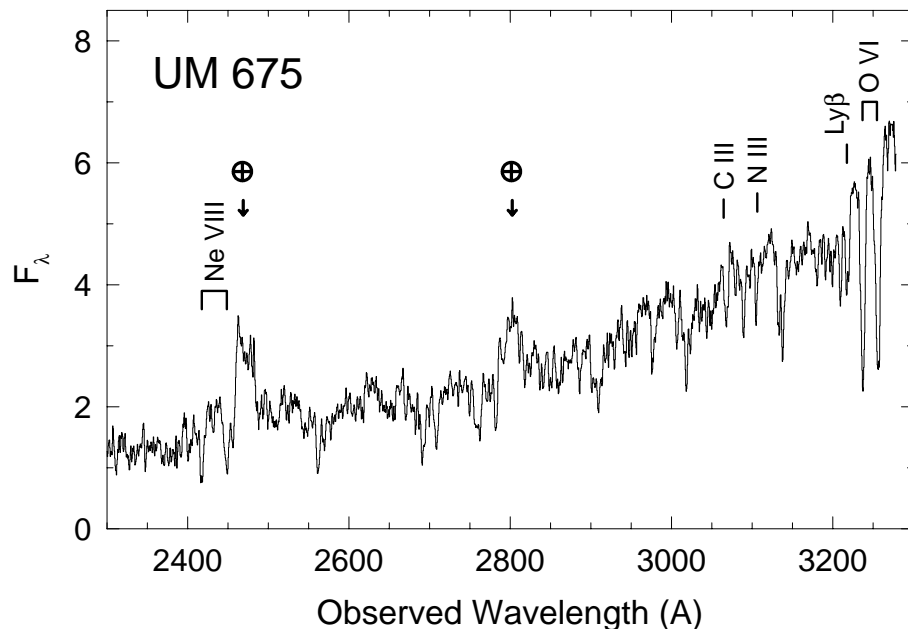


Figure 1. Pre-COSTAR *HST*-FOS spectrum of UM 675 at  $\sim 230 \text{ km s}^{-1}$  resolution. Most of the absorption lines are due to the Ly $\alpha$  forest. The strong  $z_a \approx z_e$  lines are labelled. The two marked emission features are terrestrial airglow.

We now have two firm detections of the Ne VIII doublet. Both are in  $z_a \approx z_e$  systems of redshift  $\sim 2$  QSOs: PKS 0119–046 and UM 675. All of the strong  $z_a \approx z_e$  lines in PKS 0119–046, including the Ne VIII pair, appear to be saturated and therefore do not provide accurate column densities. The results for UM 675 are more reliable. Figure 1 shows the *HST*-FOS spectrum of this source (Junkkarinen *et al.* 1997). Much higher resolution Keck Observatory spectra across the Ly $\alpha$ , C IV and N V lines are shown in Paper1 and Hamann *et al.* (1997). Table 1 lists the derived column densities ( $\log N$  in  $\text{cm}^{-2}$ ) for each of the  $z_a \approx z_e$  lines. The column densities are from Hamann *et al.* (1995) except that the metallic columns are increased by a factor of 2 to be consistent with the 50% coverage fraction derived for the C IV and N V absorbers (Paper1; Hamann *et al.* 1997). Note that this scaling is just a crude correction because different ions can cover different fractions of the background light source(s) (Hamann *et al.* 1997; Barlow & Sargent 1997).

Figure 2 plots theoretical ionization fractions,  $f(M_i)$ , for various metals, M, in ion stage,  $i$ , as a function of the ionization parameter,  $U$ , in photoionized, optically thin clouds (where  $U$  is the dimensionless ratio of hydrogen-ionizing photon to hydrogen particle densities at the illuminated face of the clouds). The H I fraction,  $f(\text{H I})$ , is shown across the top of the figure. The calculations were performed using CLOUDY (version 90.02, Ferland 1997) with an ionizing spectrum that is believed to be typical of QSOs and Seyfert 1 nuclei (from Mathews & Ferland 1987, with an additional decline at wavelengths  $\geq 2 \mu\text{m}$ ). The results do not depend on the column densities as long as the clouds are

Table 1. Example Column Densities and Abundances

Ion	$\log N(M_i)$	$[M/H]_p$	$[M/H]_{min}$
UM 675 ( $z_a \approx z_e \approx 2.14$ )			
H I	14.8	—	—
C III	14.1	$+0.4^{+0.5}_{-0.2}$	$-0.2^{+0.7}_{-0.2}$
C IV	14.9	$+0.4^{+0.7}_{-0.3}$	$-0.1^{+0.9}_{-0.3}$
N III	14.5	$+1.3^{+0.5}_{-0.2}$	$+0.7^{+0.7}_{-0.3}$
N V	15.1	$+0.3^{+0.8}_{-0.4}$	$-0.2^{+0.9}_{-0.3}$
O VI	15.5	$-0.9^{+0.8}_{-0.3}$	$-1.4^{+0.8}_{-0.3}$
Ne VIII	15.7	$-1.1^{+0.7}_{-0.4}$	$-1.4^{+0.7}_{-0.4}$
Mean BAL ( $z_e \approx 2$ )			
H I	15.4	—	—
C IV	16.0	$+1.0^{+0.7}_{-0.4}$	$+0.5^{+0.8}_{-0.4}$
N V	16.1	$+0.7^{+0.8}_{-0.4}$	$+0.5^{+0.8}_{-0.4}$
O VI	16.3:	$-0.6^{+0.7}_{-0.3}$	$-1.1^{+0.7}_{-0.4}$
Si IV	15.2	$+1.6^{+0.6}_{-0.4}$	$+1.4^{+0.6}_{-0.4}$

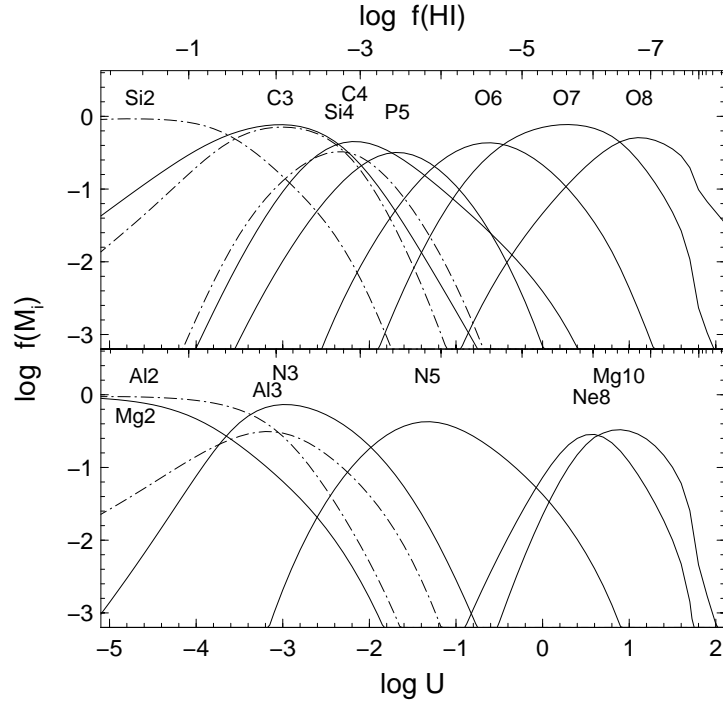


Figure 2. Ionization fractions in photoionized, optically thin clouds. The curves for each metal ion are labeled at their peaks, except for Si3, which is the dash-dot curve between Si2 and Si4 in the top panel. The notation is Si3 = Si III =  $\text{Si}^{+2}$ , etc.

optically thin in the H I Lyman continuum, as is implied by the measured column densities in most  $z_a \approx z_e$  and BAL systems – including UM 675 (Hamann 1997).

Comparing the measurements in Table 1 to the calculations in Figure 2 shows that there is a range of ionization states in the UM 675 absorber. The column density ratios of C III/C IV and N III/N V yield an abundance-independent estimate of  $U \approx 0.02$ , while the ratio O VI/Ne VIII implies  $U \approx 5$  (with the reasonable assumption that the O/Ne abundance ratio is solar). This range of ionization states requires that the clouds span factors of  $\sim 250$  in density,  $\sim 16$  in distance from the ionizing QSO, or some equivalent combination thereof.

Figure 2 also shows that we can estimate the column density in O VII+O VIII from  $N(\text{Ne VIII})$  by the relation,

$$N(\text{OVII} + \text{OVIII}) \approx N(\text{NeVIII}) \left( \frac{\text{Ne}}{\text{O}} \right) \frac{f(\text{OVII} + \text{OVIII})}{f(\text{NeVIII})} \quad (1)$$

where Ne/O is the abundance ratio and  $f(\text{Ne VIII})/f(\text{O VII}+\text{O VIII})$  is an ionization correction. For solar Ne/O and a conservatively large ionization correction factor of 10 (Fig. 2), we find  $N(\text{O VII}+\text{O VIII}) \approx 4 \times 10^{17} \text{ cm}^{-2}$ , which implies bound-free optical depths at the O VII and O VIII edges of 0.08 and 0.04, respectively. We conclude that there is highly ionized warm-absorber-like gas in the UV line forming region of UM 675, but there is not enough of that gas to actually be a warm absorber. With H. Netzer and J. Shields, we are now pursuing simultaneous observations of the Ne VIII lines and O VII+O VIII edges in other QSOs to test the UV line–X-ray warm absorber connection further.

### 3. Metal Abundances and Host Galaxy Evolution

The normalized abundance of any metal relative to hydrogen is given by,

$$\left[ \frac{\text{M}}{\text{H}} \right] = \log \left( \frac{N(\text{M}_i)}{N(\text{HI})} \right) + \log \left( \frac{f(\text{HI})}{f(\text{M}_i)} \right) + \log \left( \frac{\text{H}}{\text{M}} \right)_\odot \quad (2)$$

where  $(\text{H}/\text{M})_\odot$  is the solar abundance ratio. If the gas is in photoionization equilibrium and optically thin at all far-UV continuum wavelengths, the ionization correction factors,  $f(\text{HI})/f(\text{M}_i)$ , depend only on  $U$  and the shape of the ionizing spectrum. Column density measurements for a variety of ions can constrain  $U$  and the correction factors needed for  $[\text{M}/\text{H}]$  by comparison to Figure 2. Further comparisons to calculations using other spectral shapes can define the uncertainties (see Hamann 1997).

For systems with a range of ionization states (e.g. UM 675) or no useful constraints on  $U$ , we can derive conservatively low values of  $f(\text{HI})/f(\text{M}_i)$  and therefore  $[\text{M}/\text{H}]$  by assuming that each metal line forms where that ion is most abundant, i.e. at an ionization corresponding to the peak of its  $f(\text{M}_i)$  curve in Figure 2. We can also place firm lower limits on the  $[\text{M}/\text{H}]$  ratios by adopting the minimum ionization corrections for each  $\text{M}_i$ . Every correction factor reaches a minimum value at  $U$  values slightly larger than the peak in the  $f(\text{M}_i)$  curve. Figure 3 shows two examples of the minimum correction factors for a range of ionizing spectral shapes (from Hamann 1997). The spectra used for these calculations are segmented power laws with fixed slopes ( $f_\nu \propto \nu^\alpha$ ) of  $\alpha = -0.5$

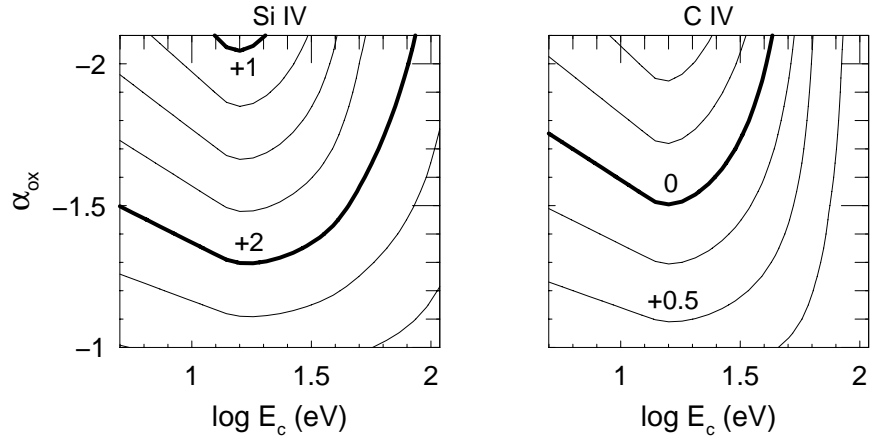


Figure 3. Contours of constant minimum ionization correction normalized by solar abundances,  $\log(f(\text{H I})/f(\text{M}_i)) + \log(\text{H}/\text{M})_\odot$ , are plotted for Si IV and C IV in optically thin clouds photoionized by a range of QSO continua. The parameters  $\alpha_{\text{ox}}$  and  $E_c$  define the continuum shapes. Bold contours appear every 1.0 dex and thin contours every 0.25 dex.

in the visible and  $-1.0$  in X-rays above  $0.7$  keV. We explore a range of continuum shapes by varying  $\alpha_{\text{ox}}$ , which relates the flux densities ( $f_\nu$ ) at  $2500 \text{ \AA}$  and  $2$  keV, and  $E_c$ , which marks the cutoff energy where the visible power law gives way to a steeper decline toward the X-ray flux at  $0.7$  keV. (This is continuum ‘C’ in Hamann 1997.) The Mathews & Ferland (1987) continuum used in Figure 2 can be approximated by  $\alpha_{\text{ox}} \approx -1.5$  and  $\log E_c \text{ (eV)} \approx 1.5$ .

The last two columns in Table 1 apply these calculations to the  $z_a \approx z_e$  absorber in UM 675 and to a set of mean column densities derived for BALs (Hamann 1997).  $[\text{M}/\text{H}]_p$  are the conservatively low abundance ratios that follow from the assumption that each metal line forms at the peak in its  $f(\text{M}_i)$  curve.  $[\text{M}/\text{H}]_{\text{min}}$  are the lower limits derived from the minimum correction factors in Figure 3 (also Hamann 1997). The uncertainties listed in the table indicate the range of values derived for a range of continuum shapes. Both  $[\text{M}/\text{H}]$  quantities are typically higher (and more realistic) for low-ionization metals because the H I lines tend to form with these ions. The  $[\text{M}/\text{H}]_p$  results provide our best guess at the actual abundances in UM 675; the overall metallicity is roughly twice solar ( $Z \approx 2 Z_\odot$ ) based on  $[\text{C}/\text{H}]$ , with nitrogen several times more enhanced. The average BAL column densities indicate that they typically have much higher metallicities of  $Z \gtrsim 25 Z_\odot$  based on  $[\text{Si}/\text{H}]$ . However, that result and the extremely high P/C ratios reported for some BALs (Turnshek *et al.* 1996 and this volume; Korista *et al.* 1996; Junkkarinen *et al.* this volume) are uncertain because the column densities depend on the unknown coverage fractions of the absorbers (also Paper1 and Arav this volume). Nonetheless, the main result for  $Z \gtrsim Z_\odot$  does appear secure and typical of all types of intrinsic absorbers (also Petitjean, Rauch & Carswell 1994; Hamann 1997). There is also independent evidence for  $Z \gtrsim Z_\odot$  in QSOs from the broad emission lines (Hamann & Ferland 1993; Ferland *et al.* 1996).

This growing evidence for high abundances in QSOs supports standard models of galaxy evolution; vigorous star formation in the spheroidal cores of massive galaxies should produce super-solar gas-phase metallicities within a few billion years of the initial collapse. High metal abundances are a signature of *massive* galaxies because only they can retain their gas long enough against the building thermal pressures from supernova explosions. The enriched gas might ultimately be ejected from the galaxy, consumed by the black hole, or diluted by subsequent infall, but the evidence for early-epoch high- $Z$  gas remains in the stars today. In particular, the mean stellar metallicities in the cores of nearby massive galaxies are typically  $\sim 1$  to  $3 Z_{\odot}$ . The individual stars are distributed about these means with metallicities reflecting the gas-phase abundance at the time of their formation. Only the most recently formed stars at any epoch have metallicities as high as that in the gas. Standard chemical evolution models indicate that the gas-phase abundances in galactic nuclei are  $\sim 2$  to  $3$  times larger than the stellar means, e.g.  $\sim 2$  to  $9 Z_{\odot}$  near the end of the star-forming epoch (see Hamann & Ferland 1993, Hamann 1997 and references therein). Therefore, metallicities in the range  $2 \lesssim Z \lesssim 9 Z_{\odot}$  can be *expected* in QSOs as long as (1) the gas we observe was processed by stars in the cores of massive ( $\gtrsim 10^{11} M_{\odot}$ ) galaxies (or at least in dense condensations that become the cores of massive galaxies), and (2) most of the star formation and enrichment occurs before the QSOs “turn on” or become observable.

**Acknowledgments.** This work was supported by NASA grants NAG 5-1630 and NAG 5-3234.

## References

- Barlow, T. A., & Sarent, W. L. W. 1997, *AJ*, 113, 136
- Ferland, G. J. 1997, *HAZY, a Brief Introduction to Cloudy*, University of Kentucky, Dept. of Physics and Astronomy, Internal Rep., in prep.
- Ferland, G. J., Baldwin, J. A., Korista, K. T., Hamann, F., Carswell, R. F., Phillips, M., Wilkes, B., & Williams, R. E. 1996, *ApJ*, 461, 683
- Hamann, F. 1997, *ApJS*, in press.
- Hamann, F., & Ferland, G. J. 1993, *ApJ*, 418, 11
- Hamann, F., Barlow, T. A., Beaver, E. A., Burbidge, E. M., Cohen, R. D., Junkkarinen, V., & Lyons, R. 1995a, *ApJ*, 443, 606
- Hamann, F., Barlow, T. A., Junkkarinen, V. T. & Burbidge, E. M. 1997, *ApJ*, 478, 80
- Junkkarinen, V., Barlow, T. A., Beaver, E. A., Burbidge, E. M., Cohen, R. D., Hamann, F., & Lyons, R. 1997, in prep.
- Korista, K. T., Hamann, F., Ferguson, J., & Ferland, G. J. 1996, *ApJ*, 461, 641
- Mathews, W. G., & Ferland, G. J. 1987, *ApJ*, 323, 456
- Mathur, S., Wilkes, B., Elvis, M., & Fiore, F. 1994, *ApJ*, 434, 493
- Petitjean, P., Rauch, M., & Carswell, R. F. 1994, *A&A*, 291, 29
- Turnshek, D. A., Kopko, M., Monier, E., Noll, D., Espey, B., & Weymann, R. J. 1996, *ApJ*, 463, 110